

Technical Note

Vibration Analysis of Axially Functionally Graded Non-Prismatic Timoshenko Beams Using the Finite Difference Method

Valentin Fogang

Civil Engineer, C/o BUNS Sarl, P.O Box 1130, Yaounde, Cameroon; valentin.fogang@bunscameroun.com

ORCID iD <https://orcid.org/0000-0003-1256-9862>

Abstract: This paper presents an approach to the vibration analysis of axially functionally graded non-prismatic Timoshenko beams (AFGNPTB) using the finite difference method (FDM). The characteristics (cross-sectional area, moment of inertia, elastic moduli, shear moduli, and mass density) of axially functionally graded beams vary along the longitudinal axis. The Timoshenko beam theory covers cases associated with small deflections based on shear deformation considerations. The FDM is an approximate method for solving problems described with differential or partial differential equations. It does not involve solving differential equations; equations are formulated with values at selected points of the structure. The model developed in this paper consists of formulating differential or partial differential equations with finite differences and introducing new points (additional or imaginary points) at boundaries and positions of discontinuity (concentrated loads or moments, supports, hinges, springs, and brutal change of stiffness). The introduction of additional points allows satisfying boundary and continuity conditions. Vibration analysis of AFGNPTB was conducted with this model, and natural frequencies were determined. Finally, the direct time integration method (DTIM) was presented. The FDM-based DTIM enabled the analysis of forced vibration of AFGNPTB, considering the damping. The efforts and displacements could be determined at any time.

Keywords: Axially functionally graded non-prismatic Timoshenko beam; finite difference method; additional points; vibration analysis; direct time integration method

1. Introduction

This paper describes the application of Fogang's model [1] based on the finite difference method, used for the Euler–Bernoulli beam, to the vibration analysis of axially functionally graded non-prismatic Timoshenko beams (AFGNPTB). Various studies have focused on the vibration analysis of AFGNPTB. Kindelan et al. [2] presented a method of obtaining optimal finite difference formulas that maximize their frequency range of validity. Both conventional and staggered equispaced stencils for first and second derivatives were considered. Mwabora et al. [3] considered numerical solutions for static and dynamic stability parameters of an axially loaded uniform beam resting on simply supported foundations using the finite difference method (FDM), where a central difference scheme was developed. Soltani et al. [4] applied the FDM to evaluate natural frequencies of non-prismatic beams with different boundary conditions and resting on variable one- or two-parameter elastic foundations. Torabi et al. [5] presented an

exact closed-form solution for free vibration analysis of Euler–Bernoulli conical and tapered beams carrying any desired number of attached masses; the concentrated masses were modeled by Dirac’s delta functions. Soltani [6] developed a semi-analytical technique to investigate the free bending vibration behavior of an axially functionally graded non-prismatic Timoshenko beam subjected to a point force at both ends, based on the power series expansion.

Classical analysis of the Timoshenko beam involves solving the governing equations (i.e., statics, dynamics, and material) that are expressed via means of differential equations, considering boundary and continuity conditions. However, solving differential equations may be difficult in the presence of an axial force (or external distributed axial forces), an elastic Winkler foundation, a Pasternak foundation, or damping (by vibration analysis). In traditional analysis using the FDM, points outside the beam are not considered. The boundary conditions are applied at the beam’s ends, not the governing equations. The non-application of governing equations at the beam’s ends leads to inaccurate results, making the FDM less useful compared with other numerical methods, such as the finite element method. This paper presented a model based on the FDM. This model consisted of formulating differential equations (statics, dynamics, and material relation) with finite differences and introducing new points (additional or imaginary points) at boundaries and at positions of discontinuity (concentrated loads or moments, supports, hinges, springs, and brutal change of stiffness). The introduction of additional points allowed us to satisfy boundary and continuity conditions. First-order, second-order, and vibration analyses of structures were also conducted using the model.

2. Materials and methods

2.1 Free vibration analysis

2.1.1 Governing equations of the free vibration

The focus here is to determine the eigenfrequencies of the beam. A second-order analysis is conducted; and the first-order analysis can easily be deduced.

The sign convention adopted for loads, bending moments, transverse forces, and displacements is illustrated in Figure 1.

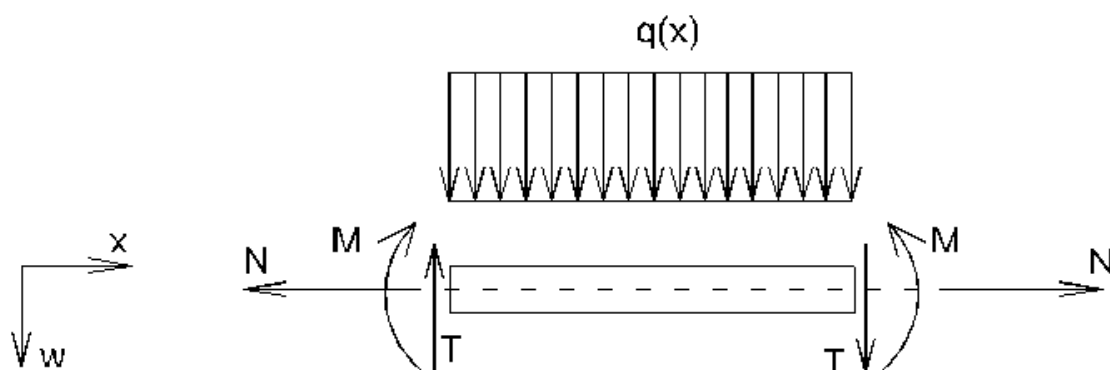


Figure 1. Sign convention for loads, bending moments, transverse forces, and displacements.

Specifically, $M(x)$ is the bending moment in the section, $T(x)$ is the transverse force, $N(x)$ is the axial force (positive in tension), $w(x)$ is the deflection, and $q(x)$ is the distributed load in the positive downward direction.

A harmonic vibration being assumed, the equations of dynamic equilibrium on an infinitesimal beam element are as follows:

$$\frac{dT(x)}{dx} - k(x)w(x) + \omega^2 \rho(x)A(x)w(x) = 0 \quad (1a)$$

$$\frac{dM(x)}{dx} + N(x)\frac{dw(x)}{dx} - T(x) - \omega^2 \rho(x)I(x)\varphi(x) = 0 \quad (1b)$$

where $\rho(x)$ is the beam's mass per unit volume, $A(x)$ is the cross-sectional area, $I(x)$ is the moment of inertia, $k(x)$ is the stiffness of the elastic Winkler foundation, $\varphi(x)$ is the rotation (positive in clockwise) of the cross section, and ω is the circular frequency of the beam.

The transverse force $T(x)$ is related to the shear force $V(x)$, as follows:

$$T(x) = V(x) + N(x)\frac{dw(x)}{dx} \quad (2)$$

Let us consider an external distributed axial load $n(x)$ positive along the + x axis

$$n(x) = -\frac{dN(x)}{dx} \quad (3)$$

Substituting Equations (2) and (3) into Equations (1a-b) yields

$$\frac{dV(x)}{dx} + N(x)\frac{d^2w(x)}{dx^2} - n(x)\frac{dw(x)}{dx} - k(x)w(x) + \omega^2 \rho(x)A(x)w(x) = 0 \quad (4a)$$

$$\frac{dM(x)}{dx} - V(x) - \omega^2 \rho(x)I(x)\varphi(x) = 0 \quad (4b)$$

According to the Timoshenko beam theory, the bending moment and shear force are related to the deflection and rotation of the cross section $\varphi(x)$, as follows:

$$M(x) = -E(x)I(x)\frac{d\varphi(x)}{dx} \quad (5a) \quad V(x) = \kappa G(x)A(x) \times \left(\frac{dw(x)}{dx} - \varphi(x) \right) \quad (5b)$$

Where at a position x , $E(x)$ is the elastic modulus, $G(x)$ is the shear modulus, and κ is the shear correction factor.

Substituting Equations (5a-b) into Equations (4a-b) yields

$$\frac{d[\kappa G(x)A(x)]}{dx} \times \left(\frac{dw(x)}{dx} - \varphi(x) \right) + \kappa G(x)A(x) \times \left(\frac{d^2w(x)}{dx^2} - \frac{d\varphi(x)}{dx} \right) + \quad (6a)$$

$$N(x)\frac{d^2w(x)}{dx^2} - n(x)\frac{dw(x)}{dx} - k(x)w(x) + \omega^2 \rho(x)A(x)w(x) = 0$$

(6b)

$$\frac{d[E(x)I(x)]}{dx} \times \frac{d\varphi(x)}{dx} + E(x)I(x)\frac{d^2\varphi(x)}{dx^2} + \kappa G(x)A(x) \times \left(\frac{dw(x)}{dx} - \varphi(x) \right) + \omega^2 \rho(x)I(x)\varphi(x) = 0$$

2.1.2 Fundamentals of the FDM

Let us consider a segment k of the beam having equidistant grid points with spacing h_k .

Equations (6a-b) have a second-order derivative; consequently, the deflection and rotation curves $w(x)$, and $\varphi(x)$, respectively, are approximated around the point of interest i as second-degree polynomials.

Thus, a three-point stencil is used to write finite difference approximations to derivatives at grid points. The derivatives ($S(x)$ representing $w(x)$ or $\varphi(x)$) at i are expressed with deflection values at points $i-1$, i , and $i+1$.

$$\left. \frac{d^2 S(x)}{dx^2} \right|_i = \frac{S_{i-1} - 2S_i + S_{i+1}}{h_k^2} \quad (7a)$$

$$\left. \frac{dS(x)}{dx} \right|_i = \frac{-S_{i-1} + S_{i+1}}{2h_k} \quad (7b)$$

2.1.3 FDM Formulation of equations and efforts

Since the characteristics of the beam vary throughout the longitudinal axis, reference values are defined. The reference values of the beam's mass per unit volume, the cross-sectional area, the moment of inertia, the elastic modulus, and the shear modulus are denoted by ρ_r , A_r , I_r , E_r , and G_r , respectively. At a position x the beam's mass per unit volume, the cross-sectional area, the moment of inertia, the elastic modulus, and the shear modulus are related to the reference values as follows:

$$\rho(x) = \beta_\rho(x) \times \rho_r \quad (8a)$$

$$E(x) = \beta_E(x) \times E_r \quad (8d)$$

$$A(x) = \beta_A(x) \times A_r \quad (8b)$$

$$G(x) = \beta_G(x) \times G_r \quad (8e)$$

$$I(x) = \beta_I(x) \times I_r \quad (8c)$$

The reference length is denoted by l_r . The bending shear factor α_r and other parameters are defined as follows:

$$\alpha_r = E_r I_r / (\kappa G_r A_r l_r^2) \quad (9a)$$

$$W(x) = E_r I_r \times w(x) \quad (9c)$$

$$h_k = \beta_{lk} l_r \quad (9b)$$

$$\Phi(x) = E_r I_r \times \varphi(x) \quad (9d)$$

The following parameters describing the rate of change of stiffnesses $E(x)I(x)$ and $\kappa G(x)A(x)$ are defined as follows:

$$\beta'_{GA}(x) = h_k \frac{d[\beta_G(x)\beta_A(x)]}{dx} \quad (10a)$$

$$\beta'_{EI}(x) = h_k \frac{d[\beta_E(x)\beta_I(x)]}{dx} \quad (10b)$$

The reference coefficient of rotary inertia k_{RIr} and the vibration frequency ω are defined as follows:

$$k_{RIr} = \frac{I_r}{A_r l_r^2} \quad (11a)$$

$$\omega = \lambda \times \sqrt{\frac{E_r I_r}{\rho_r A_r l_r^4}} \quad (11b)$$

Substituting Equations (7a-b), (8a-e), (9a-d), (10a-b), and (11a-b) into Equations (6a-b) yields the FDM formulations of the governing equations as follows:

$$\begin{aligned} & \left(-\frac{\beta'_{GAi}\beta_{lk}^2}{2\alpha_r} + \frac{\beta_{Gi}\beta_{Ai}\beta_{lk}^2}{\alpha_r} + \frac{N_i h_k^2}{E_r I_r} + \frac{n_i h_k^3}{2E_r I_r} \right) W_{i-1} - \left(\frac{2\beta_{Gi}\beta_{Ai}\beta_{lk}^2}{\alpha_r} + \frac{2N_i h_k^2}{E_r I_r} + \frac{k_i h_k^4}{E_r I_r} - \beta_{\rho i}\beta_{Ai}\beta_{lk}^4 \lambda^2 \right) W_i \\ & + \left(\frac{\beta'_{GAi}\beta_{lk}^2}{2\alpha_r} + \frac{\beta_{Gi}\beta_{Ai}\beta_{lk}^2}{\alpha_r} + \frac{N_i h_k^2}{E_r I_r} - \frac{n_i h_k^3}{2E_r I_r} \right) W_{i+1} + \frac{\beta_{Gi}\beta_{Ai}\beta_{lk}^2}{2\alpha_r} h_k \Phi_{i-1} - \frac{\beta'_{GAi}\beta_{lk}^2}{\alpha_r} h_k \Phi_i - \frac{\beta_{Gi}\beta_{Ai}\beta_{lk}^2}{2\alpha_r} h_k \Phi_{i+1} = 0 \end{aligned} \quad (12a)$$

$$\begin{aligned} & -\frac{\beta_{Gi}\beta_{Ai}\beta_{lk}^2}{2\alpha_r} W_{i-1} + \frac{\beta_{Gi}\beta_{Ai}\beta_{lk}^2}{2\alpha_r} W_{i+1} + \left(\beta_{Ei}\beta_{li} - \frac{\beta'_{Eli}}{2} \right) h_k \Phi_{i-1} - \left(2\beta_{Ei}\beta_{li} + \frac{\beta_{Gi}\beta_{Ai}\beta_{lk}^2}{\alpha_r} - k_{Rlr}\beta_{\rho i}\beta_{li}\beta_{lk}^2 \lambda^2 \right) h_k \Phi_i \\ & + \left(\beta_{Ei}\beta_{li} + \frac{\beta'_{Eli}}{2} \right) h_k \Phi_{i+1} = 0 \end{aligned} \quad (12b)$$

Equations (12a-b) are the governing equations. Substituting Equations (7b), (8b-e), and (9a-d) into Equations (2) and (5a-b) yields the bending moment and transverse force, as follows:

$$M_i = \beta_{Ei}\beta_{li} \frac{\Phi_{i-1} - \Phi_{i+1}}{2h_k} \quad (13a)$$

$$T_i = -\frac{1}{h_k^3} \left(\frac{\beta_{Gi}\beta_{Ai}\beta_{lk}^2}{2\alpha_r} + \frac{N_i h_k^2}{2E_r I_r} \right) W_{i-1} + \frac{1}{h_k^3} \left(\frac{\beta_{Gi}\beta_{Ai}\beta_{lk}^2}{2\alpha_r} + \frac{N_i h_k^2}{2E_r I_r} \right) W_{i+1} - \frac{1}{h_k^3} \frac{\beta_{Gi}\beta_{Ai}\beta_{lk}^2}{\alpha_r} h_k \Phi_i \quad (13b)$$

For the special case of an AFGNPTB without an axial force or a Winkler foundation, Equation (12a) becomes

$$\begin{aligned} & \left(-\frac{\beta'_{GAi}\beta_{lk}^2}{2\alpha_r} + \frac{\beta_{Gi}\beta_{Ai}\beta_{lk}^2}{\alpha_r} \right) W_{i-1} - \left(\frac{2\beta_{Gi}\beta_{Ai}\beta_{lk}^2}{\alpha_r} - \beta_{\rho i}\beta_{Ai}\beta_{lk}^4 \lambda^2 \right) W_i \\ & + \left(\frac{\beta'_{GAi}\beta_{lk}^2}{2\alpha_r} + \frac{\beta_{Gi}\beta_{Ai}\beta_{lk}^2}{\alpha_r} \right) W_{i+1} + \frac{\beta_{Gi}\beta_{Ai}\beta_{lk}^2}{2\alpha_r} h_k \Phi_{i-1} - \frac{\beta'_{GAi}\beta_{lk}^2}{\alpha_r} h_k \Phi_i - \frac{\beta_{Gi}\beta_{Ai}\beta_{lk}^2}{2\alpha_r} h_k \Phi_{i+1} = 0 \end{aligned} \quad (14)$$

The shear force is then calculated as follows:

$$V_i = \frac{\beta_{Gi}\beta_{Ai}\beta_{lk}^2}{\alpha_r h_k^3} \left(-\frac{W_{i-1}}{2} + \frac{W_{i+1}}{2} - h_k \Phi_i \right) \quad (15)$$

2.1.3 Analysis at beam's ends and at positions of discontinuity

Positions of discontinuity are positions of concentrated mass, spring–mass system, supports, hinges, springs, abrupt change in cross section, positions where $E(x)I(x)$ and $\kappa G(x)A(x)$ are not differentiable, and change in grid spacing. The model used in this paper (developed in Fogang [1]) consists of realizing an opening of the beam at the position of discontinuity and introducing additional points (imaginary points i_a and i_d) in the opening, as represented in Figure 2. Imaginary points are also introduced at beam's ends (points 0 and $n+2$), so governing equations are applied at the beam's ends, as well as boundary conditions.

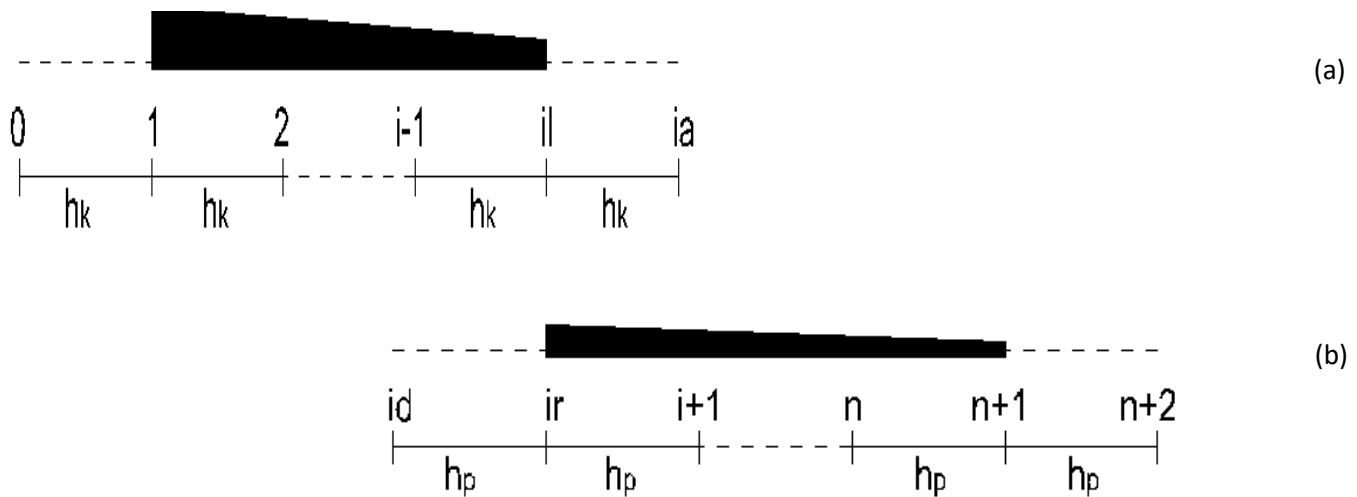


Figure 2. Introduction of imaginary points at beam's ends and in the opening at the left side (a) and right side (b).

Thus, the governing equations (Equations (12a-b)) are applied at any point on the grid (1, 2, ..., $i-1$, i_l , i_r , $i+1$, ..., $n+1$) of Figure 2). The continuity equations express the continuity of the deflection and rotation of the cross section, and the equilibrium of bending moments and transverse forces. The continuity equations for deflections, rotations of the cross sections, and bending moments are defined as follows:

$$w_{i_l} = w_{i_r} \rightarrow W_{i_l} = W_{i_r} \quad (16a)$$

$$\varphi_{i_l} = \varphi_{i_r} \rightarrow \Phi_{i_l} = \Phi_{i_r} \quad (16b)$$

$$M_{i_l} - M_{i_r} = 0 \rightarrow \beta_{Eil} \beta_{Iil} \frac{\Phi_{i-1} - \Phi_{i_a}}{2h_k} - \beta_{Eir} \beta_{Iir} \frac{\Phi_{i_d} - \Phi_{i+1}}{2h_p} = 0 \quad (16c)$$

An adjustment of the continuity equations is made e.g. in the case of a hinge (no continuity of the rotation of the cross section; $M_{i_l} = M_{i_r} = 0$), a support ($W_{i_l} = W_{i_r} = 0$, no balance of transverse forces), or a spring.

The equilibrium of transverse forces depends on the case of discontinuity. The transverse forces T_{i_l} and T_{i_r} in Equations (17), (19), and (20a) are calculated using Equation (13b).

Effect of a concentrated force P_i : The balance of vertical forces yields

$$T_{il} - T_{ir} - P_i = 0 \quad (17)$$

Effect of a concentrated mass: The dynamic behavior of a beam carrying a concentrated mass M_p was analyzed. We set

$$M_p = m_p \times \rho_r A_r l_r \quad (18)$$

Applying Equations (9c), (11b), and (18), the balance of vertical forces yields

$$T_{il} - T_{ir} - \frac{M_p \omega^2}{E_r I_r} W_{il} = 0 \rightarrow T_{il} - T_{ir} - \frac{m_p}{l_r^3} \lambda^2 W_{il} = 0 \quad (19)$$

Effect of a spring–mass system: The dynamic behavior of a beam carrying a spring–mass system was analyzed.

The deflection of the mass is denoted by W_{iM} . The spring stiffness K_p is defined as follows:

$$K_p = k_p \times E_r I_r / l_r^3 \quad (20)$$

Applying Equations (9c), (11b), (18), and (20), the balance of vertical forces yields

$$T_{il} - T_{ir} - \frac{M_p \omega^2}{E_r I_r} W_{iM} = 0 \rightarrow T_{il} - T_{ir} - \frac{m_p}{l_r^3} \lambda^2 W_{iM} = 0 \quad (21a)$$

$$\frac{M_p \omega^2}{E_r I_r} W_{iM} = \frac{K_p}{E_r I_r} \times (W_{iM} - W_{ir}) \rightarrow m_p \lambda^2 W_{iM} = k_p (W_{iM} - W_{ir}) \quad (21b)$$

2.2 Direct time integration method

The direct time integration method used here (developed in Fogang [1]) describes the dynamic response of a beam as a multi-degree-of-freedom system. Viscosity η and external loading $p(x,t)$ are considered. The equations of dynamic equilibrium on an infinitesimal beam element are as follows:

$$\frac{d\kappa GA(x)}{dx} \left(\frac{\partial w^*(x,t)}{\partial x} - \varphi^*(x,t) \right) + \kappa GA(x) \left(\frac{\partial^2 w^*(x,t)}{\partial x^2} - \frac{\partial \varphi^*(x,t)}{\partial x} \right) \quad (21a)$$

$$-n(x) \frac{\partial w^*(x,t)}{\partial x} + N(x) \frac{\partial^2 w^*(x,t)}{\partial x^2} - k(x) w^*(x,t) - \rho A(x) \frac{\partial^2 w^*(x,t)}{\partial t^2} - \eta \frac{\partial w^*(x,t)}{\partial t} = -p(x,t) \quad (21b)$$

$$\frac{dEI(x)}{dx} \frac{\partial \varphi^*(x,t)}{\partial x} + EI(x) \frac{\partial^2 \varphi^*(x,t)}{\partial x^2} + \kappa GA(x) \times \left(\frac{\partial w^*(x,t)}{\partial x} - \varphi^*(x,t) \right) - \rho I(x) \frac{\partial^2 \varphi^*(x,t)}{\partial t^2} = 0$$

The derivatives with respect to x are formulated using Equations (7a-b), while those with respect to t (time increment is Δt) are formulated considering a three-point stencil with Equations (22a-c):

$$\left. \frac{\partial w^*(x,t)}{\partial t} \right|_{i,t} = \frac{-w^*_{i,t-\Delta t} + w^*_{i,t+\Delta t}}{2\Delta t} \quad \left. \frac{\partial^2 w^*(x,t)}{\partial t^2} \right|_{i,t} = \frac{w^*_{i,t-\Delta t} - 2w^*_{i,t} + w^*_{i,t+\Delta t}}{\Delta t^2} \quad (22a)$$

At initial time $t = 0$, a three-point forward difference approximation is applied:

$$\left. \frac{\partial^2 w^*}{\partial t^2} \right|_{i,0} = \frac{w^*_{i,0} - 2w^*_{i,\Delta t} + w^*_{i,2\Delta t}}{\Delta t^2} \quad \left. \frac{\partial w^*}{\partial t} \right|_{i,0} = \frac{-3w^*_{i,0} + 4w^*_{i,\Delta t} - w^*_{i,2\Delta t}}{2\Delta t} \quad (22b)$$

At final time $t = T$, a three-point backward difference approximation is applied:

$$\left. \frac{\partial^2 w^*}{\partial t^2} \right|_{i,T} = \frac{w^*_{i,T-2\Delta t} - 2w^*_{i,T-\Delta t} + w^*_{i,T}}{\Delta t^2} \quad \left. \frac{\partial w^*}{\partial t} \right|_{i,T} = \frac{w^*_{i,T-2\Delta t} - 4w^*_{i,T-\Delta t} + 3w^*_{i,T}}{2\Delta t} \quad (22c)$$

The governing equations (Equations (21a-b)) can be formulated with the FDM for $x = i$ at time t . The FDM formulations of these equations are applied at any point of the beam at any time t using a five-point stencil. Additional points are introduced to satisfy the boundary and continuity conditions. The boundary conditions are satisfied using a three-point stencil. Thus, beam deflection $w^*(x,t)$ and rotation $\phi^*(x,t)$ can be determined with the Cartesian model represented in Figure 3. The bending moment $M^*(x,t)$ and transverse force $T^*(x,t)$ are calculated using Equations (13a-b).

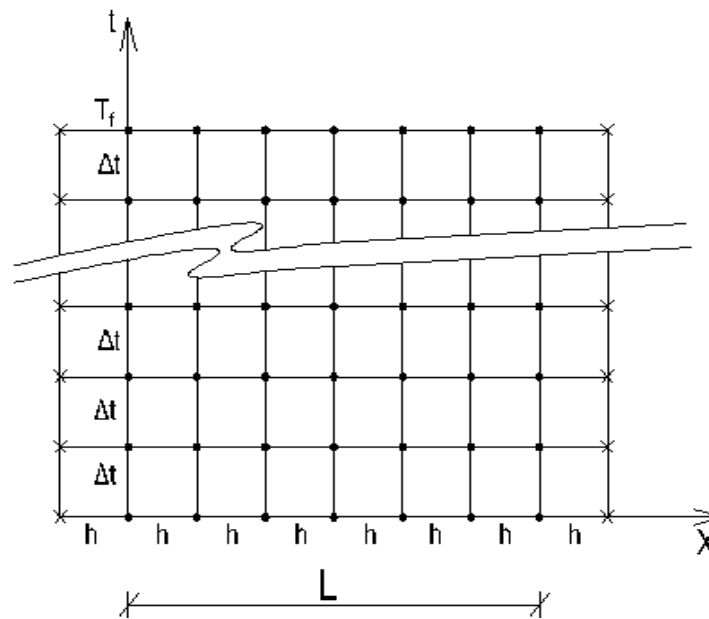


Figure 3. Model for the calculation of time-dependent vibration of a axially functionally graded beam.

3 Results and discussion

3.1 Free vibration analysis of AFG tapered Timoshenko beams

We determined the vibration frequencies (coefficients λ) of axially functionally graded non-prismatic (AFGNP) Timoshenko beams. Pinned–pinned, fixed–free, and fixed–fixed beams were considered. Soltani [6] presented results obtained with the power series method (PSM) and those obtained by Shahba et al. [7] with the finite element method (FEM). Case B of [6], described as follows, is considered: the height and breadth of the beam vary linearly in longitudinal axis with same tapering ratio $\beta = 1 - h_0/h_1 = 1 - b_0/b_1$. The heights and breadths at the left and the right beam's end, respectively, are denoted by h_0 , b_0 , h_1 , b_1 .

The beams have the following characteristics: Poisson's ratio $\nu = 0.30$, Timoshenko shear coefficient $\kappa = 5/6$, and coefficient of rotary inertia $k_{RI} = 0.01$.

The reference values ρ_r , A_r , I_r , E_r , and G_r are taken at the left beam's end.

$$I(x) = I_r(1-\beta x/l)^4, A(x) = A_r(1-\beta x/l)^2, E_r = 200 \text{ GPa}, \rho_r = 5700 \text{ kg/m}^3, E_1 = 70 \text{ GPa}, \rho_1 = 2702 \text{ kg/m}^3$$

$$E(x) = E_r + (E_1 - E_r)(x/l)^2, \rho(x) = \rho_r + (\rho_1 - \rho_r)(x/l)^2$$

FDM Analysis was conducted with $n = 9, 17, 33$, and 49 grid points for different values of the taper ratio and support conditions. Detailed results are listed in Appendix A and in the Supplementary Material "Vibration analysis of AFG tapered Timoshenko beams."

The results of this study are compared with the results of Soltani [6] and Shahba et al. [7] in Table 1.

Table 1. Coefficients λ of natural frequencies (first mode) of AFGNP Timoshenko beams Case B: power series method (PSM), Shahba et al. [7], and FDM.

Taper ratio	PSM	Shahba et al. [7], FEM	FDM 9-pt grid	FDM 17-pt grid	FDM 33-pt grid	FDM 49-pt grid
Fixed–free beam						
0.2	4.2390	4.2384	4.2497	4.2394	4.2384	4.2382
0.5	5.0170	5.0178	4.8744	4.9753	5.0057	5.0116
Pinned–pinned beam						
0.2	7.2246	7.2245	7.50588	7.2901	7.2390	7.2297
0.5	5.7128	5.7118	5.8261	5.7072	5.7050	5.7059
Fixed–fixed beam						
0.2	12.2385	12.2429	12.8558	12.3996	12.2779	12.2551
0.5	11.3145	11.3199	12.09198	11.5094	11.3600	11.3325

The results of this study have high accuracy.

4 Conclusion

The FDM-based model developed in this paper enables, with relative easiness, vibration analysis of axially functionally graded non-prismatic Timoshenko beams. The results show that the calculations, as described in this paper, yield accurate results.

The following aspects were not addressed in this study but could be analyzed with the model in the future:

- ✓ Axially functionally graded Timoshenko beams resting on Pasternak foundations
- ✓ Elastically connected multiple-beam system

Supplementary Materials: The following files were uploaded during submission:

- “Vibration analysis of AFG tapered Timoshenko beams”

Funding:

Acknowledgments:

Conflicts of Interest: The author declares no conflict of interest.

Appendix A: Vibration analysis of AFG tapered Timoshenko beams

The bending shear factor (Equation (9a)) is calculated as follows

$$\alpha = \frac{E_r I_r}{\kappa G_r A_r l_r^2} = \frac{1}{\kappa} \times \frac{E_r}{G_r} \times \frac{I_r}{A_r l_r^2} = \frac{1}{5/6} \times 2(1+0.30) \times 0.01 = 0.0312 \quad (\text{A1})$$

The parameters $\beta_I(x)$, $\beta_A(x)$, $\beta_\rho(x)$, $\beta_E(x)$, $\beta_G(x)$, $\beta'_{GA}(x)$, and $\beta'_{EI}(x)$ are calculated as follows:

$$\begin{aligned} \beta_I(x) &= [1 - \beta x/l]^4 & \beta_A(x) &= [1 - \beta x/l]^2 & \beta_\rho(x) &= 1 + (\rho_1/\rho_0 - 1) \times (x/l)^2 \\ \beta_E(x) &= \beta_G(x) = 1 + (E_1/E_0 - 1) \times (x/l)^2 & & & & \\ \beta'_{GA}(x) &= h_k \frac{d[\beta_G(x)\beta_A(x)]}{dx} = & & & & \\ & 2(E_1/E_0 - 1) \times (x/l) \beta_{lk} [1 - \beta x/l]^2 - 2[1 + (E_1/E_0 - 1) \times (x/l)^2] \beta \beta_{lk} (1 - \beta x/l) & & & & \\ \beta'_{EI}(x) &= h_k \frac{d[\beta_E(x)\beta_I(x)]}{dx} = & & & & \\ & 2(E_1/E_0 - 1) \times (x/l) \beta_{lk} [1 - \beta x/l]^4 - 4[1 + (E_1/E_0 - 1) \times (x/l)^2] \beta \beta_{lk} [1 - \beta x/l]^3 & & & & \end{aligned} \quad (\text{A2})$$

References

- [1] Fogang, V. Euler-Bernoulli Beam Theory: First-Order Analysis, Second-Order Analysis, Stability, and Vibration Analysis Using the Finite Difference Method. Preprints 2021, 2021020559 (doi: 10.20944/preprints202102.0559.v2).
- [2] M. Kindelan, M. Moscoso, P. Gonzalez-Rodriguez. Optimized Finite Difference Formulas for Accurate High Frequency Components. *Mathematical Problems in Engineering*. Volume 2016, Article ID 7860618, 15 pages. <http://dx.doi.org/10.1155/2016/7860618>
- [3] Mwabora, K. O.; Sigey, J. K.; Okelo, J. A.; Giterere, K. A numerical study on transverse vibration of Euler–Bernoulli beam. *IJESIT*, Volume 8, Issue 3, May 2019
- [4] M. Soltani, A. Sistani, B. Asgarian. Free Vibration Analysis of Beams with Variable Flexural Rigidity Resting on one or two Parameter Elastic Foundations using Finite Difference Method. Conference Paper. The 2016 World Congress on The 2016 Structures Congress (Structures16)
- [5] K. Torabi, H. Afshari, M. Sadeghi, H. Toghian. Exact Closed-Form Solution for Vibration Analysis of Truncated Conical and Tapered Beams Carrying Multiple Concentrated Masses. *Journal of Solid Mechanics* Vol. 9, No. 4 (2017) pp. 760-782
- [6] Soltani, M: Vibration characteristics of axially loaded tapered Timoshenko beams made of functionally graded materials by the power series method. *Numerical Methods in Civil Engineering*. July 2017. DOI:[10.29252/nmce.2.1.1](https://doi.org/10.29252/nmce.2.1.1)
- [7] Shahba A., Attarnejad R., Tavanaie Marvi M., Hajilar S. (2011). “Free vibration and stability analysis of axially functionally graded tapered Timoshenko beams with classical and non-classical boundary conditions.” *Composites: Part B*, 42 (4), 801-808.